Table S1. Molecular properties and Drug likeness score of *Drymaria cordata* phytochemicals.

S. No.	Bioactives	MF	MW	NHBA	NHBD	Mol. Vol (A^3)	DLS
1	2,4 DNP (2,4 Dinitrophenyl hydrazine)	$C_6H_6N_4O_4$	198.04	5	3	145.74	-1.78
2	2,4 D (2,4 Dichloro phenoxy acetic acid)	$C_8H_6C_{12}O_3$	219.97	3	1	171.10	-0.64
3	2,3,6-Trichlorobenzoic acid	$C_7H_3Cl_3O_2$	223.92	2	1	157.45	-1.18
4	Drymaritin	$C_{15}H_{10}N_2O_2$	250.07	3	0	260.08	-0.60
5	1,6-anhydro-β-D-Glucopyranose	$C_6H_{10}O_5$	162.05	5	3	128.62	-1.17
6	L-Gala-L-Ido-Octose	$C_8H_{16}O_8$	240.08	8	7	198.27	-0.42
7	3,7,11,15-tetramethyle-2-hexabecen-1-ol	$C_{20}H_{40}O$	296.31	1	1	372.58	-0.87
8	n-hexadecanoic acid	$C_{16}H_{32}O_2$	256.24	2	1	305.93	-0.54
9	9,12-Octadicadienoic acid, methyl ester	$C_{18}H_{32}O_2$	280.24	2	1	353.96	-0.30
10	Oleyl alcohol	$C_{18}H_{36}O$	268.28	1	1	344.00	-1.11
11	17- octa decynoic acid	$C_{18}H_{32}O_2$	280.24	2	1	342.70	-0.15
12	1,1 –diphenyl-2-picrylhydrazyl	$C_{18}H_{13}N_5O_6$	395.09	6	1	327.30	-1.33
13	Stigmasterol	$C_{29}H_{48}O$	412.37	1	1	529.89	0.62
14	quercetin 3-O-β-D-glucopyranosyl-(1->2)-rhamnopyranoside	$C_{27}H_{30}O_{16}$	610.15	16	10	533.87	0.88
15	24-ethyl-cholesta-5,22E-dien-3β-O-β-D-glucopyranosyle	$C_{37}H_{62}O_6$	602.45	6	4	703.47	0.47
16	digalactosyldiacylglycerol	$C_{49}H_{88}O_{15}$	916.61	15	7	972.05	0.16
17	Cyclohaxen 1,4,5-triol-3-one-1-Carboxylic acid	$C_7H_{10}O_6$	190.05	6	4	177.83	-0.77
18	[(2S,3S,4R,8E)-2N-[(2')-2'-hydroxylpentaeicosanoyl]-8(E)-tetraeicosanoyl-1, 3, 4-triol]	$C_{49}H_{97}NO_5$	779.74	5	5	935.92	-0.97
19	(2S,3R,4E,8E,2'R)-1-O-β-D-glucopyranosyl-2- (2-hydroxypalmitoyl)-amino-4,8-octadecadien-1,3-diol	$C_{26}H_{49}NO_9$	519.34	10	8	528.72	-0.33
20	5,4'-dihydroxy-7-methoxyflavone-6-C – (2''-O-α-L-rhamnopyranosyl)-β-D-glucopyranoside	$C_{28}H_{32}O_{15}$	608.17	15	9	536.36	0.90
21	5,7,3' ,4' -tetrahydroxyflavone-6-C-(2''-O-α-L-rhamnopyranosyl)-β-D-glucopyranoside	$C_{27}H_{30}O_{16}$	610.15	16	11	529.09	0.81
22	Cassiaoccidentalin A	$C_{26}H_{26}O_{15}$	578.13	15	9	506.04	0.94

MF: Molecular formula, MW: Molecular weight, NHBA- Number of Hydrogen Bond Donor, NHBD- Number of Hydrogen Bond Acceptor, DLS- Drug likeness Score

Table S2. Toxicity analysis of selected phytochemicals.

Phytocompounds	Hepatotoxicity	Carcinogenicity	Mutagenicity	Cytotoxicity
Stigmasterol	Inactive	Inactive	Inactive	Inactive
24-ethyl-cholesta-5,22E-dien-3β-O-β-D-glucopyranosyle	Inactive	Inactive	Inactive	Inactive
5,4'-dihydroxy-7-methoxyflavone-6-C –(2''-O-α -L-rhamnopyranosyl)-β-D-glucopyranoside	Inactive	Inactive	Inactive	Inactive
quercetin 3-O-β-D-glucopyranosyl-(1->2)-rhamnopyranoside	Inactive	Inactive	Inactive	Inactive
5,7,3' ,4' -tetrahydroxyflavone-6-C-(2''-O-α-L-rhamnopyranosyl)-β-D-glucopyranoside	Inactive	Inactive	Inactive	Inactive
Cassiaoccidentalin A	Inactive	Inactive	Inactive	Inactive

Table S3. Binding free energy components for the quercetin 3-O-β-D-glucopyranosyl-(1->2)-rhamnopyranosidecomplexed with 4QAF and 7JII proteins calculated by MM-GBSA.

Energies (kcal/mol)	**4QAF+ quercetin 3-O-β-D-glucopyranosyl-(1->2)-rhamnopyranoside**	**7JII+ quercetin 3-O-β-D-glucopyranosyl-(1->2)-rhamnopyranoside**
ΔG_{bind}	-76.04±2.63	-85.26±2.99
ΔG_{bind}Lipo	-23.96±1.03	-31.50±3.1
ΔG_{bind}vdW	-51.10±2.0	-70.63±2.63
ΔG_{bind}Coulomb	-8.12±1.99	-43.66±2.88
$\Delta G_{bind}H_{bond}$	-0.41±0.22	-1.87±0.5
ΔG_{bind}SolvGB	16.5±1.09	60.54±2.8
ΔG_{bind}Covalent	1.56±1.2	4.22±1.07

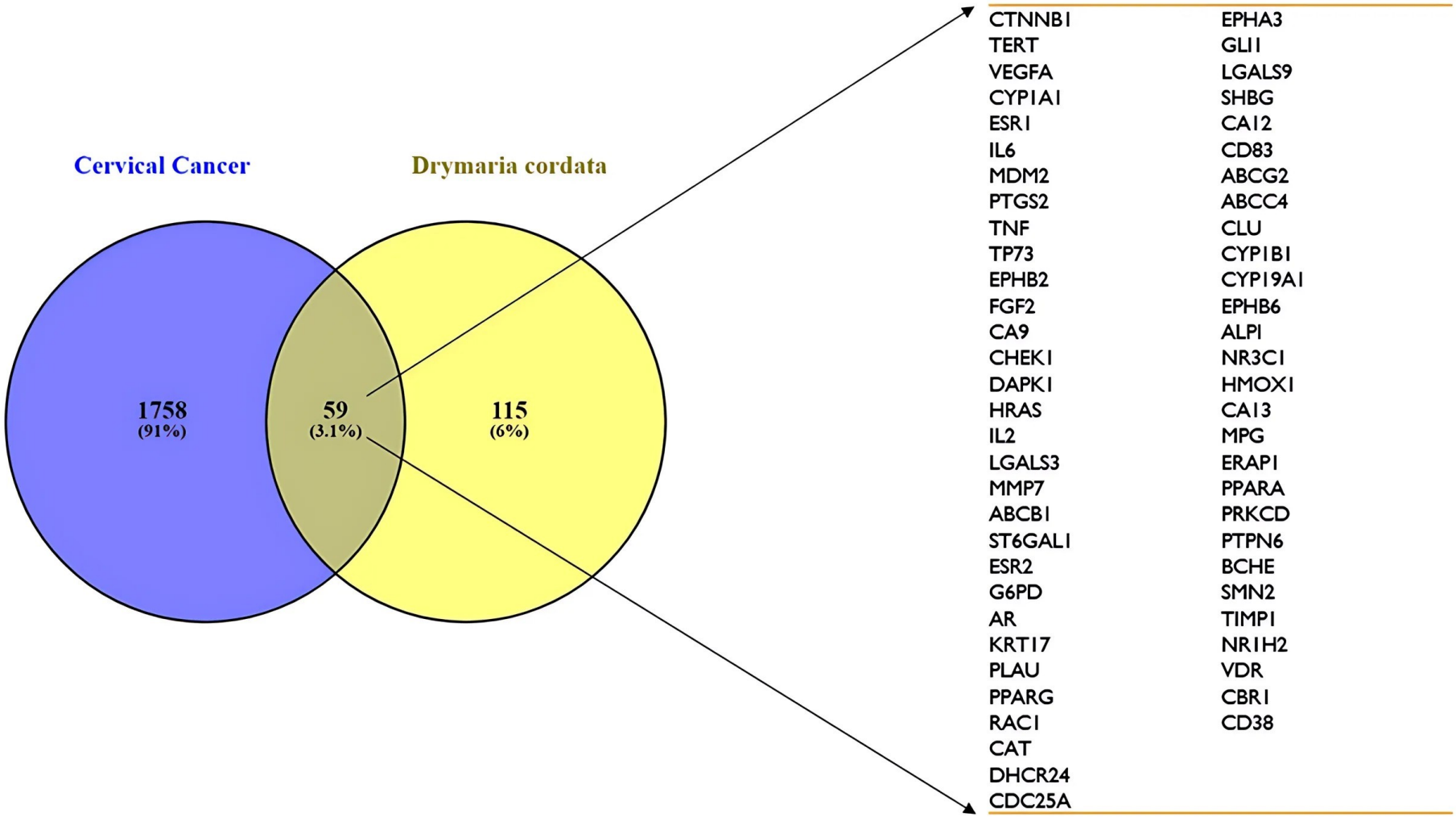

Figure S1. Venn Diagram of Cervical cancer genes and genes interacted by phytochemicals of *Drymaria cordata.*

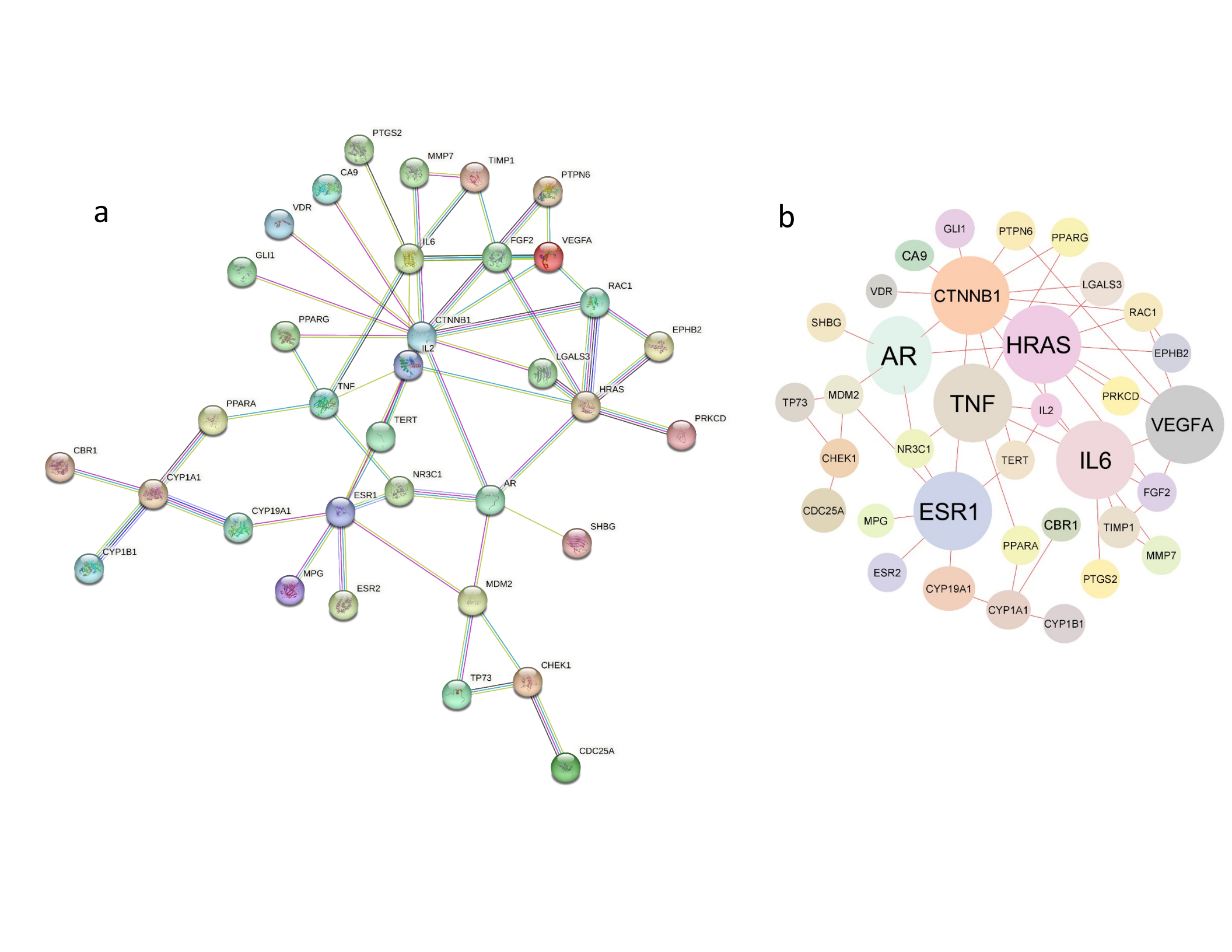
a
PTGS2
MMP7
TIMP1
CA9
PTPN6
VDR
IL6
FGF2
VEGFA
GLI1
RAC1
PPARG
CTNNB1
EPHB2
IL2
LGALS3
TNF
HRAS
PPARA
TERT
PRKCD
CBR1
CYP1A1
NR3C1
AR
ESR1
CYP19A1
SHBG
CYP1B1
MPG
ESR2
MDM2
CHEK1
TP73
CDC25A
b
GLI1
PTPN6
PPARG
CA9
VDR
CTNNB1
LGALS3
RAC1
SHBG
AR
HRAS
EPHB2
TP73
MDM2
TNF
PRKCD
IL2
VEGFA
CHEK1
NR3C1
TERT
IL6
FGF2
CDC25A
MPG
ESR1
CBR1
TIMP1
PPARA
MMP7
ESR2
CYP19A1
PTGS2
CYP1A1
CYP1B1

Figure S2. a: Protein-protein interaction (visualized in a: STRING and b: Cytoscape after analysis) of the phytochemicals-triggered proteins. Node color;  colored nodes: query proteins and first shell of interactors,  filled nodes: some 3D structure is known or predicted, Known Interactions;  from curated databases,  experimentally determined, Predicted Interactions;  gene neighbourhood,  gene fusions,  gene co-occurrence & Others;  text mining,  co-expression,  protein homology.

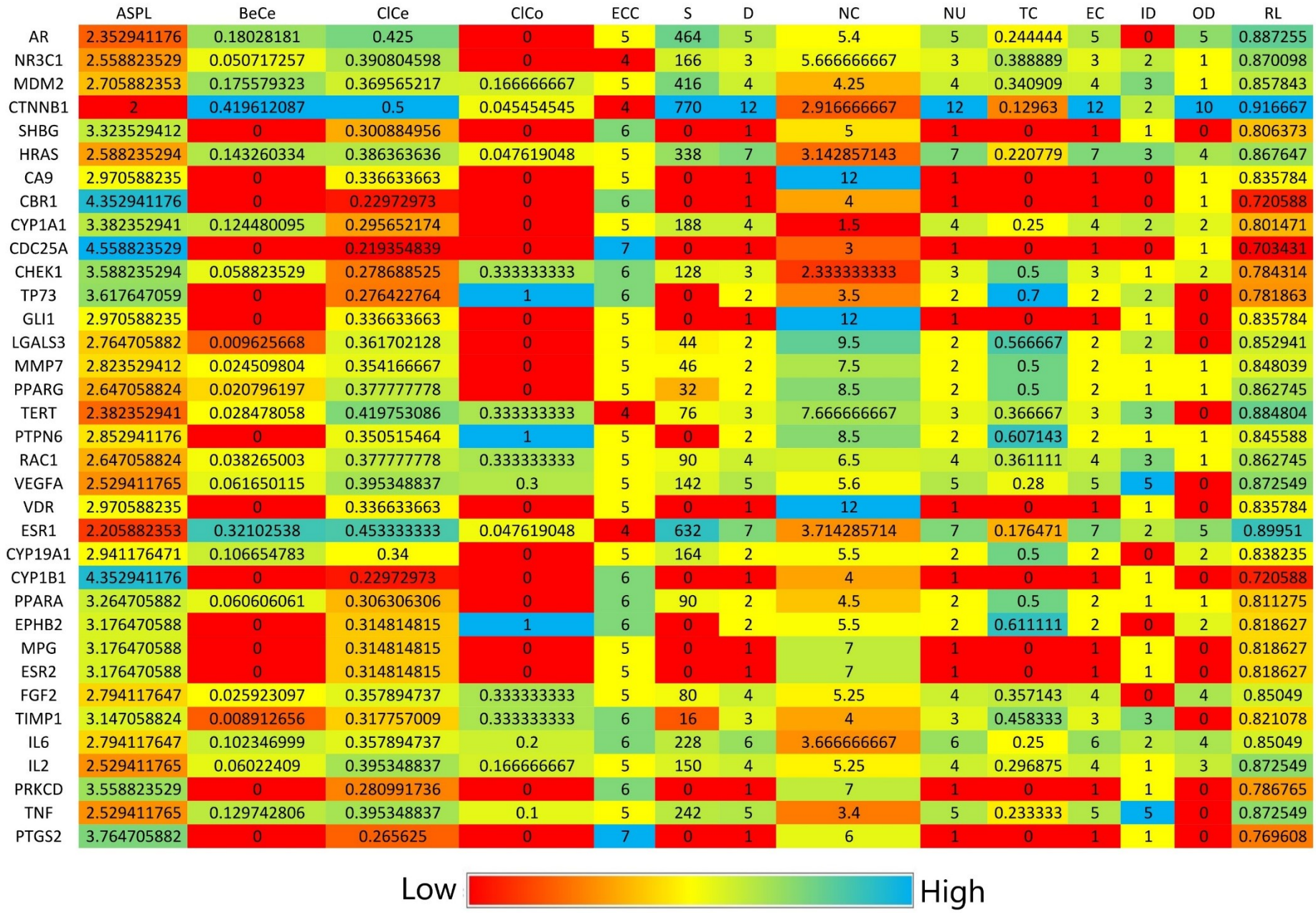

	ASPL	BeCe	ClCe	ClCo	ECC	S	D	NC	NU	TC	EC	ID	OD	RL
AR	2.352941176	0.18028181	0.425	0	5	464	5	5.4	5	0.244444	5	0	5	0.887255
NR3C1	2.558823529	0.050717257	0.390804598	0	4	166	3	5.666666667	3	0.388889	3	2	1	0.870098
MDM2	2.705882353	0.175579323	0.369565217	0.166666667	5	416	4	4.25	4	0.340909	4	3	1	0.857843
CTNNB1	2	0.419612087	0.5	0.045454545	4	770	12	2.916666667	12	0.12963	12	2	10	0.916667
SHBG	3.323529412	0	0.300884956	0	6	0	1	5	1	0	1	1	0	0.806373
HRAS	2.588235294	0.143260334	0.386363636	0.047619048	5	338	7	3.142857143	7	0.220779	7	3	4	0.867647
CA9	2.970588235	0	0.336633663	0	5	0	1	12	1	0	1	0	1	0.835784
CBR1	4.352941176	0	0.22972973	0	6	0	1	4	1	0	1	0	1	0.720588
CYP1A1	3.382352941	0.124480095	0.295652174	0	5	188	4	1.5	4	0.25	4	2	2	0.801471
CDC25A	4.558823529	0	0.219354839	0	7	0	1	3	1	0	1	0	1	0.703431
CHEK1	3.588235294	0.058823529	0.278688525	0.333333333	6	128	3	2.333333333	3	0.5	3	1	2	0.784314
TP73	3.617647059	0	0.276422764	1	6	0	2	3.5	2	0.7	2	2	0	0.781863
GLI1	2.970588235	0	0.336633663	0	5	0	1	12	1	0	1	1	0	0.835784
LGALS3	2.764705882	0.009625668	0.361702128	0	5	44	2	9.5	2	0.566667	2	2	0	0.852941
MMP7	2.823529412	0.024509804	0.354166667	0	5	46	2	7.5	2	0.5	2	1	1	0.848039
PPARG	2.647058824	0.020796197	0.377777778	0	5	32	2	8.5	2	0.5	2	1	1	0.862745
TERT	2.382352941	0.028478058	0.419753086	0.333333333	4	76	3	7.666666667	3	0.366667	3	3	0	0.884804
PTPN6	2.852941176	0	0.350515464	1	5	0	2	8.5	2	0.607143	2	1	1	0.845588
RAC1	2.647058824	0.038265003	0.377777778	0.333333333	5	90	4	6.5	4	0.361111	4	3	1	0.862745
VEGFA	2.529411765	0.061650115	0.395348837	0.3	5	142	5	5.6	5	0.28	5	5	0	0.872549
VDR	2.970588235	0	0.336633663	0	5	0	1	12	1	0	1	1	0	0.835784
ESR1	2.205882353	0.32102538	0.453333333	0.047619048	4	632	7	3.714285714	7	0.176471	7	2	5	0.89951
CYP19A1	2.941176471	0.106654783	0.34	0	5	164	2	5.5	2	0.5	2	0	2	0.838235
CYP1B1	4.352941176	0	0.22972973	0	6	0	1	4	1	0	1	1	0	0.720588
PPARA	3.264705882	0.060606061	0.306306306	0	6	90	2	4.5	2	0.5	2	1	1	0.811275
EPHB2	3.176470588	0	0.314814815	1	6	0	2	5.5	2	0.611111	2	0	2	0.818627
MPG	3.176470588	0	0.314814815	0	5	0	1	7	1	0	1	1	0	0.818627
ESR2	3.176470588	0	0.314814815	0	5	0	1	7	1	0	1	1	0	0.818627
FGF2	2.794117647	0.025923097	0.357894737	0.333333333	5	80	4	5.25	4	0.357143	4	0	4	0.85049
TIMP1	3.147058824	0.008912656	0.317757009	0.333333333	6	16	3	4	3	0.458333	3	3	0	0.821078
IL6	2.794117647	0.102346999	0.357894737	0.2	6	228	6	3.666666667	6	0.25	6	2	4	0.85049
IL2	2.529411765	0.06022409	0.395348837	0.166666667	5	150	4	5.25	4	0.296875	4	1	3	0.872549
PRKCD	3.558823529	0	0.280991736	0	6	0	1	7	1	0	1	1	0	0.786765
TNF	2.529411765	0.129742806	0.395348837	0.1	5	242	5	3.4	5	0.233333	5	5	0	0.872549
PTGS2	3.764705882	0	0.265625	0	7	0	1	6	1	0	1	1	0	0.769608

Low High

Figure S3. Score analysis of each protein for different protein nodes. ASPL: average short path length, *BeCe*: Betweenness Centrality, *ClCo*: clustering coefficient, *ClCe*: closeness centrality, *ECC*: eccentricity, *S*: stress, *D*: Degree, *NC*: neighbourhood connectivity, *NU*: Number of Undirected Edges, *TC*: Topological Coefficient, *EC*: Edge count, *ID*: In degree, *OD*: Outdegree, *RL*: Radiality.

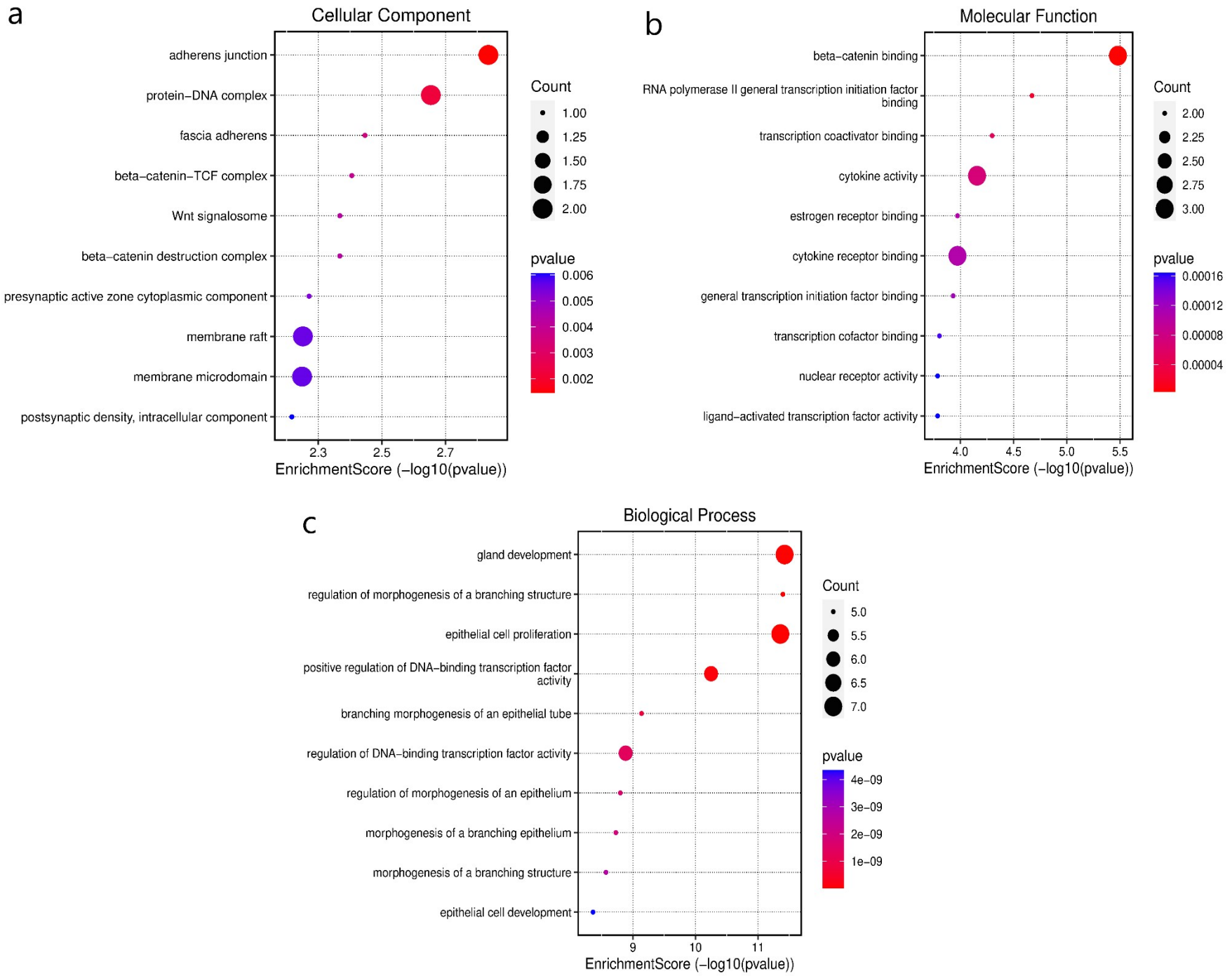
a
Cellular Component
adherens junction
protein−DNA complex
fascia adherens
beta−catenin−TCF complex
Wnt signalosome
beta−catenin destruction complex
presynaptic active zone cytoplasmic component
membrane raft
membrane microdomain
postsynaptic density, intracellular component
2.3
2.5
2.7
EnrichmentScore (−log10(pvalue))
Count
1.00
1.25
1.50
1.75
2.00
pvalue
0.006
0.005
0.004
0.003
0.002
b
Molecular Function
beta−catenin binding
RNA polymerase II general transcription initiation factor binding
transcription coactivator binding
cytokine activity
estrogen receptor binding
cytokine receptor binding
general transcription initiation factor binding
transcription cofactor binding
nuclear receptor activity
ligand−activated transcription factor activity
4.0
4.5
5.0
5.5
EnrichmentScore (−log10(pvalue))
Count
2.00
2.25
2.50
2.75
3.00
pvalue
0.00016
0.00012
0.00008
0.00004
c
Biological Process
gland development
regulation of morphogenesis of a branching structure
epithelial cell proliferation
positive regulation of DNA−binding transcription factor activity
branching morphogenesis of an epithelial tube
regulation of DNA−binding transcription factor activity
regulation of morphogenesis of an epithelium
morphogenesis of a branching epithelium
morphogenesis of a branching structure
epithelial cell development
9
10
11
EnrichmentScore (−log10(pvalue))
Count
5.0
5.5
6.0
6.5
7.0
pvalue
4e−09
3e−09
2e−09
1e−09

Figure S4. Gene ontology analysis of hub genes for cellular components, molecular function, and biological process. The gene ontology terms were evaluated at 5 percent false discovery rate stringency for Homo sapiens.

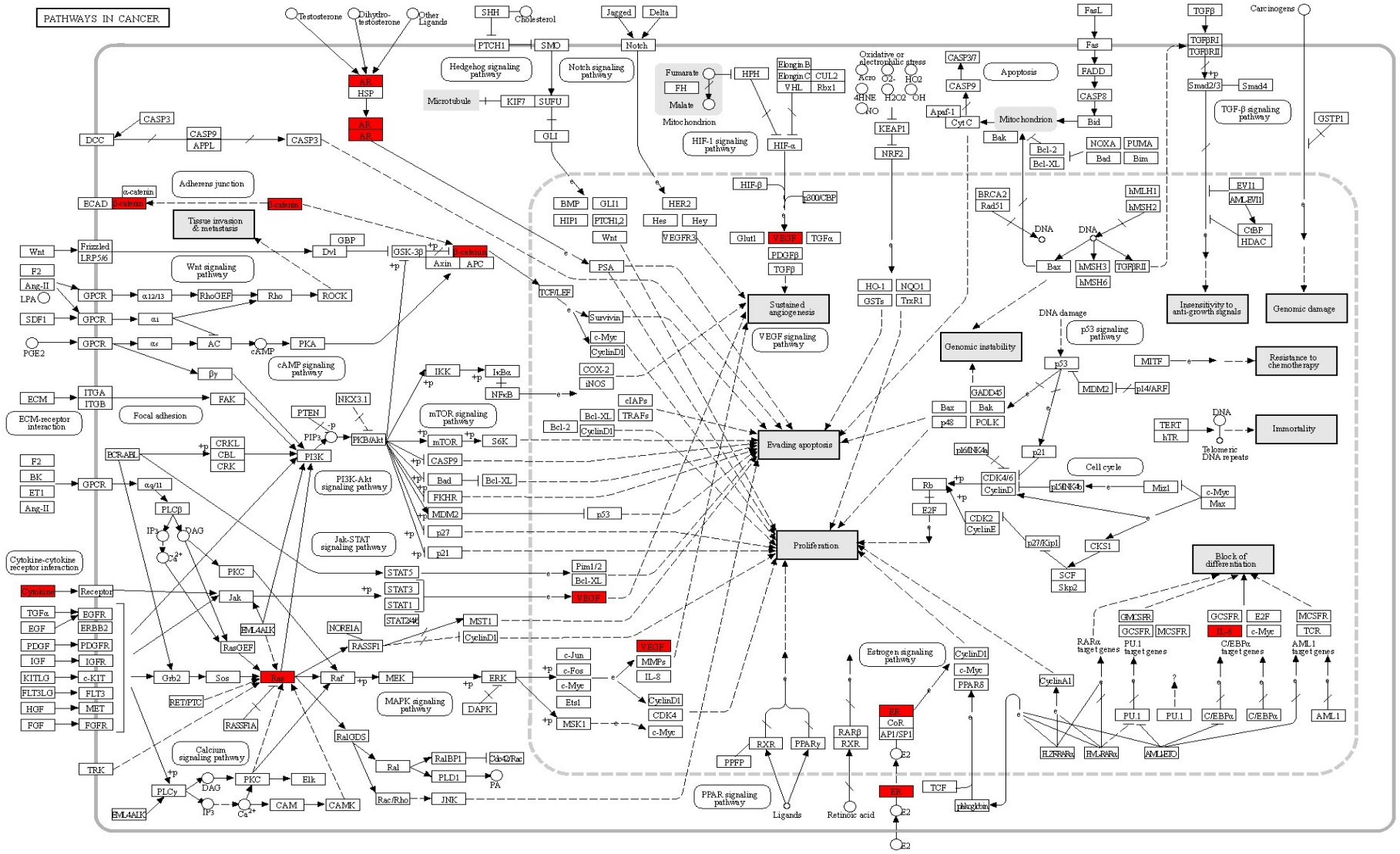

Figure S5. KEGG pathway analysis of Hub genes marked in red color

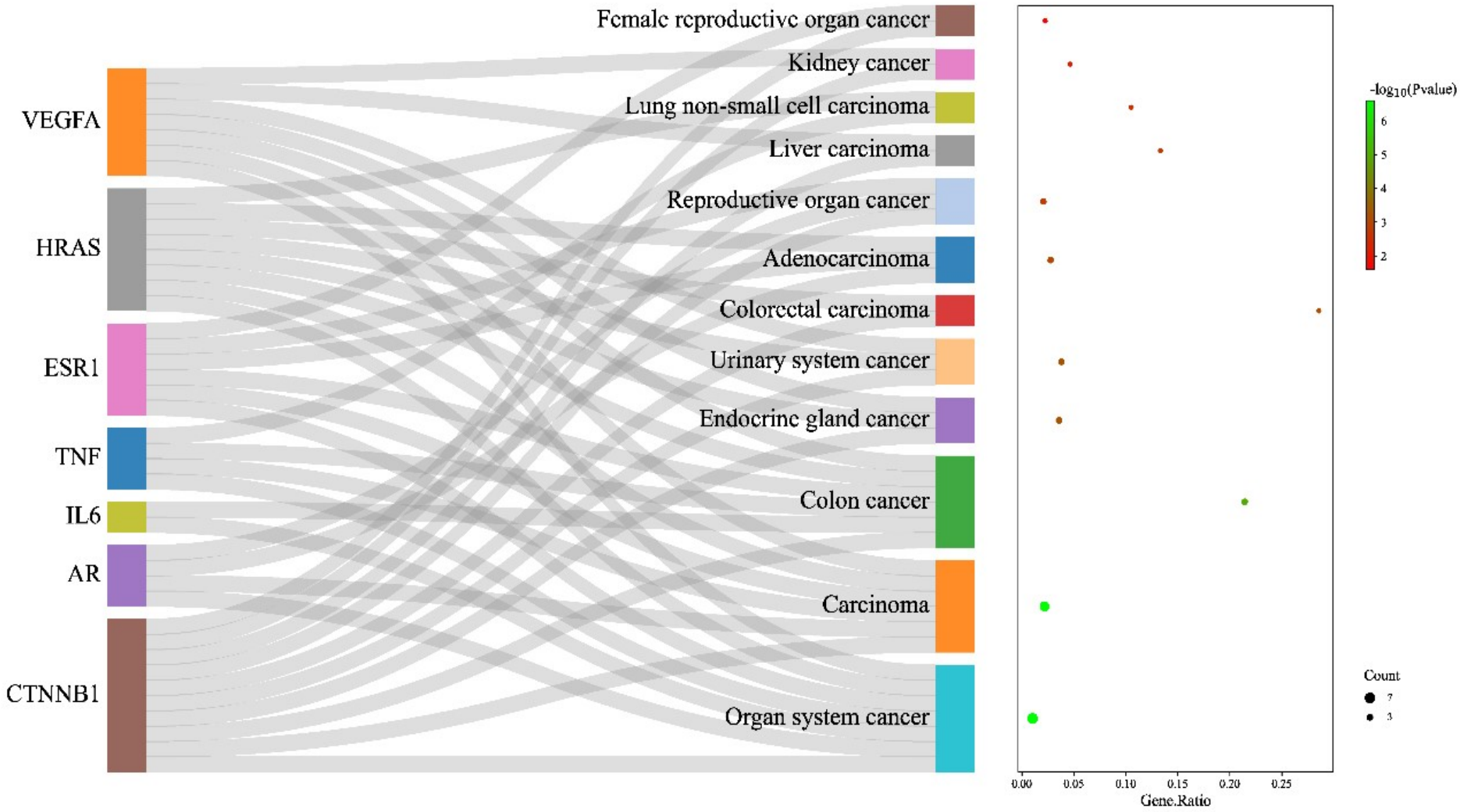

Figure S6. Interaction representation of the disease–gene association. The interaction was evaluated at a 5 % false discovery rate stringency for *Homo sapiens* against a whole genome statistical background run.

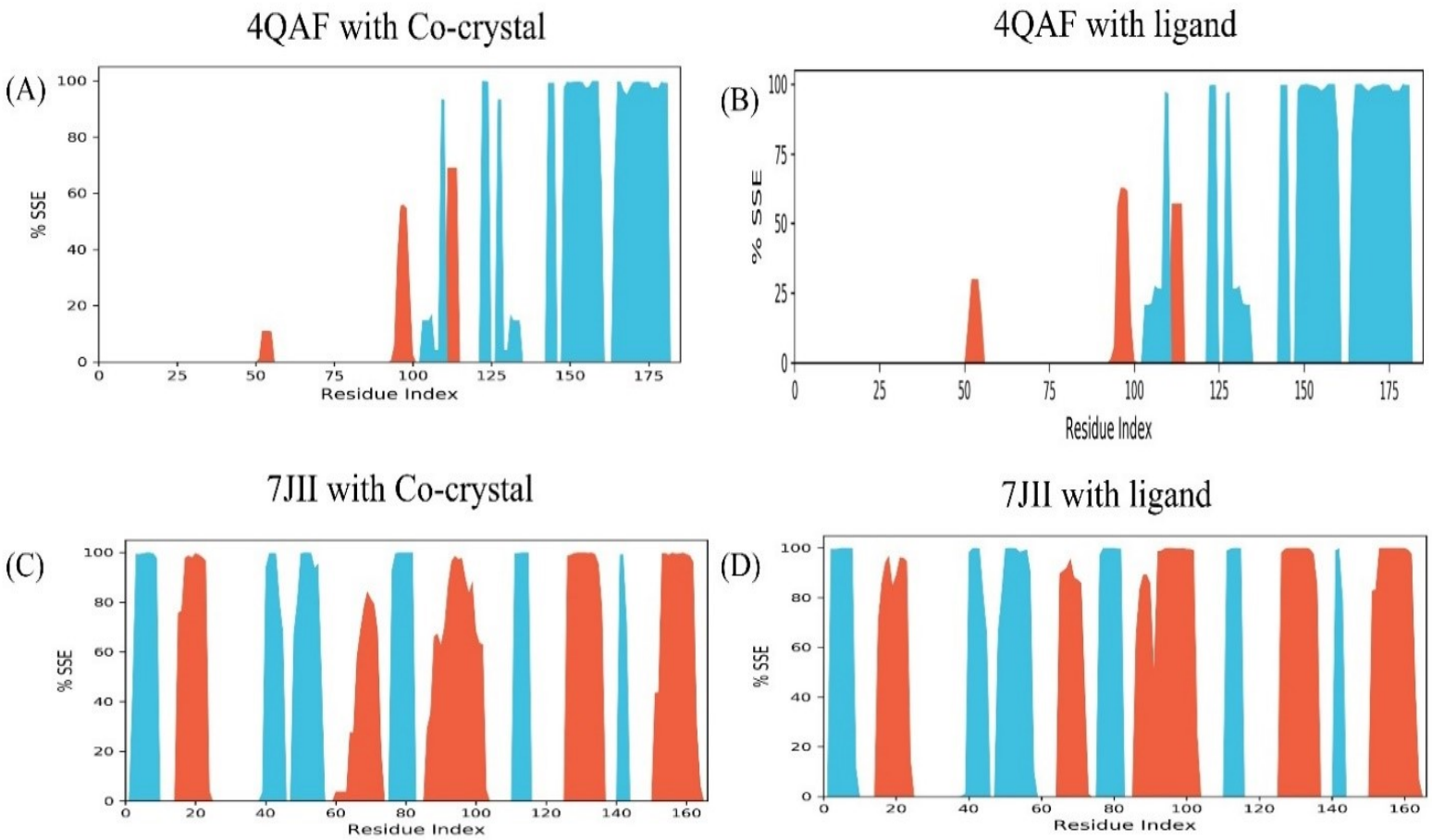

Figure S7. The distribution of protein-co-crystallized ligands and the protein-quercetin 3-O-β-D-glucopyranosyl-(1->2)-rhamnopyranoside complex forms secondary structural elements by residue index across the protein structure. The graph illustrates the distribution of SSE based on the index of each residue within the protein's structure. The α-helices are indicated by red color, β-strands are indicated by blue color, and the loop regions are indicated by white.

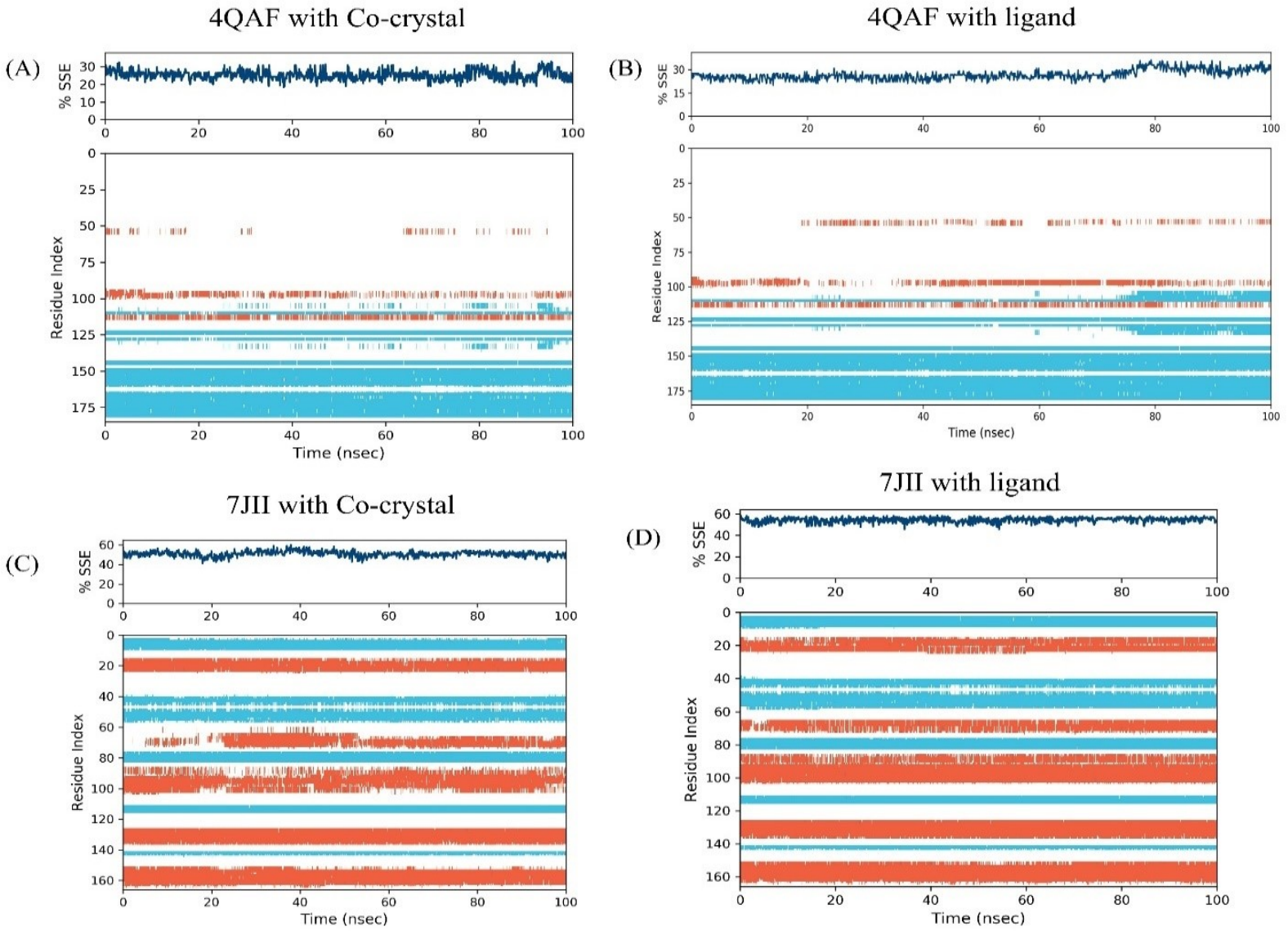
4QAF with Co-crystal
(A)
% SSE
Residue Index
Time (nsec)
4QAF with ligand
(B)
% SSE
Residue Index
Time (nsec)
7JII with Co-crystal
(C)
% SSE
Residue Index
Time (nsec)
7JII with ligand
(D)
% SSE
Residue Index
Time (nsec)

Figure S8. Evolution of secondary structure over the 100 ns simulation time and participation of different residues in the secondary structure. Alpha helices are indicated by red color, β-strands are indicated by light blue color, and the loop regions are indicated by white color in protein-co-crystallized ligand complexes and complexes with quercetin 3-O-β-D-glucopyranosyl-(1->2)-rhamnopyranoside.

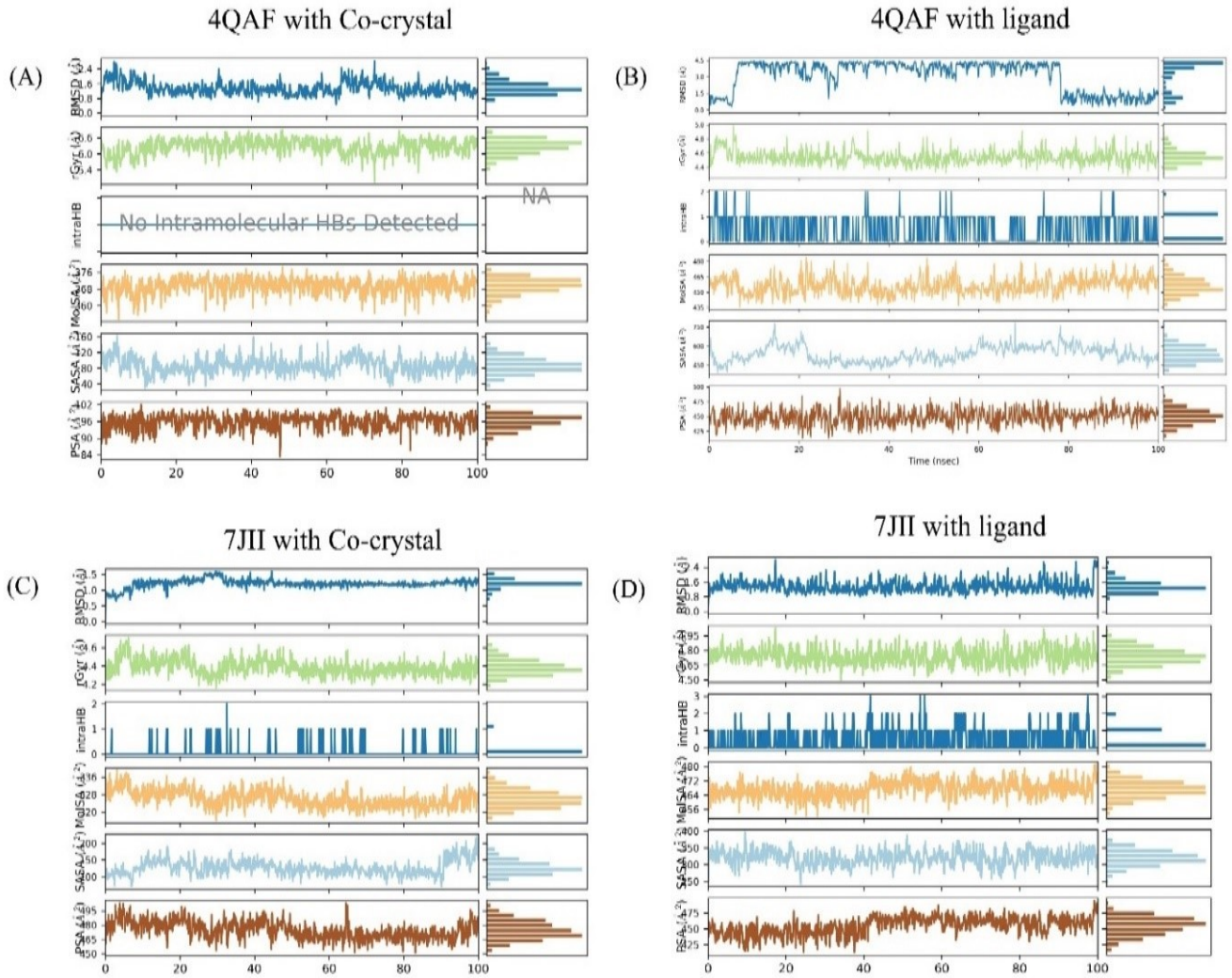

Figure S9. Ligand property analysis of VEGF with (A) co-crystallized ligand and (B) quercetin 3-O-β-D-glucopyranosyl-(1->2)-rhamnopyranoside, HRAS with (C) co-crystallized ligand and (D) quercetin 3-O-β-D-glucopyranosyl-(1->2)-rhamnopyranoside for 100 ns of molecular dynamics simulation time. RMSD: Root mean square deviation of a ligand concerning the reference conformation (typically the first frame is used as the reference and is regarded as time t = 0). rGyr: Measures the 'extendedness' of a ligand and is

equivalent to its principal moment of inertia. intraHB: Number of internal hydrogen bonds within a ligand molecule. MolSA: Molecular surface calculation with a 1.4 Å probe radius. This value is equivalent to a van der Waals surface area. SASA: Surface area of a molecule accessible by a water molecule. PSA: Solvent-accessible surface area in a molecule contributed only by oxygen and nitrogen atoms.

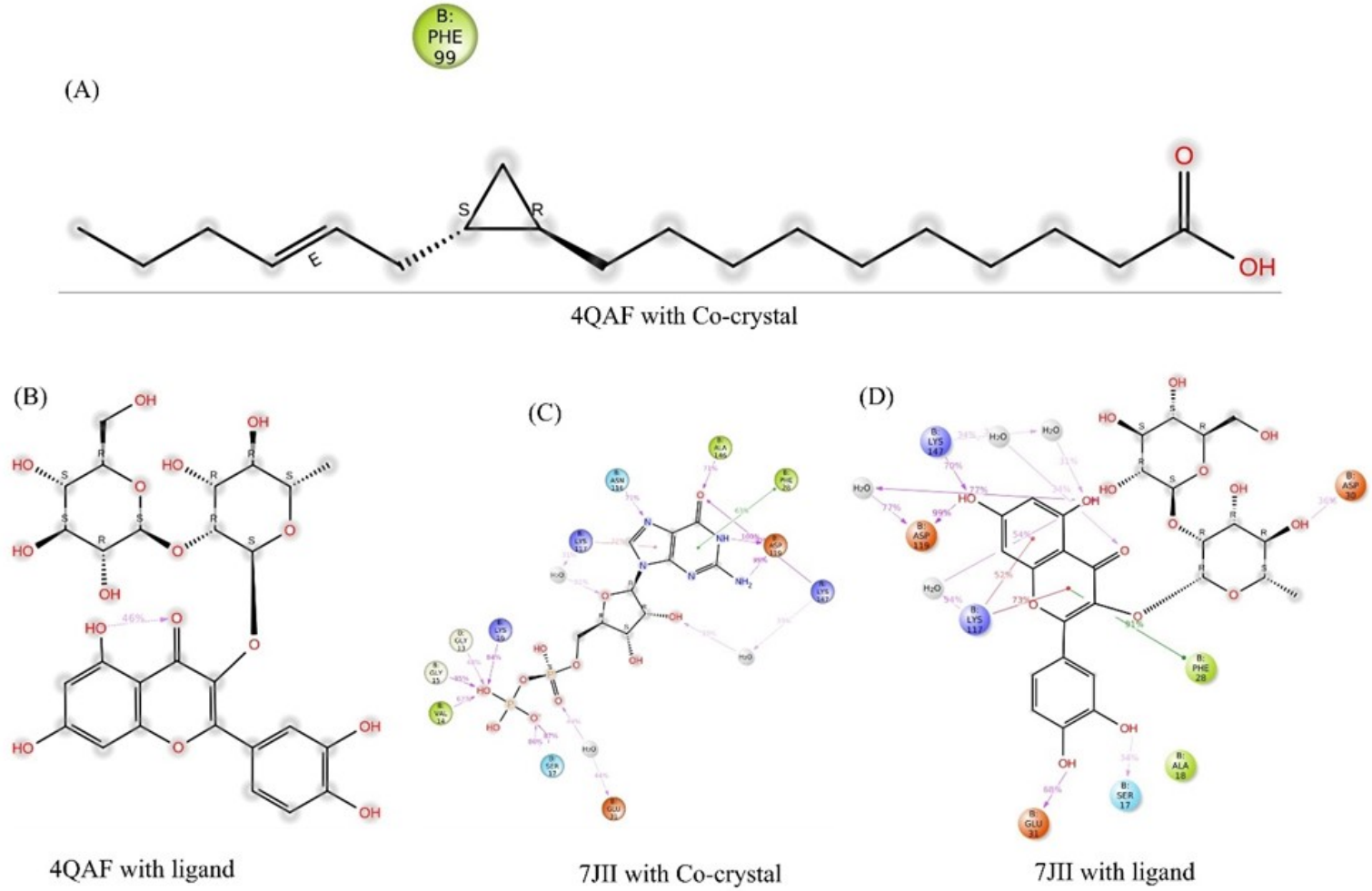

Figure S10. 2D interaction plot from post dynamics trajectories of(A) VEGF+Co-crystallized ligand (B) VEGF+quercetin 3-O-β-D-glucopyranosyl-(1->2)-rhamnopyranoside and (C) HRAS+Co-crystallized ligand (D) HRAS+quercetin 3-O-β-D-glucopyranosyl-(1->2)-rhamnopyranoside. The diagrams illustrates the intricate interactions between ligand atoms and protein residues. Only interactions occurring for over 30.0% of the simulation duration within the chosen trajectory (0–100 ns) are depicted.

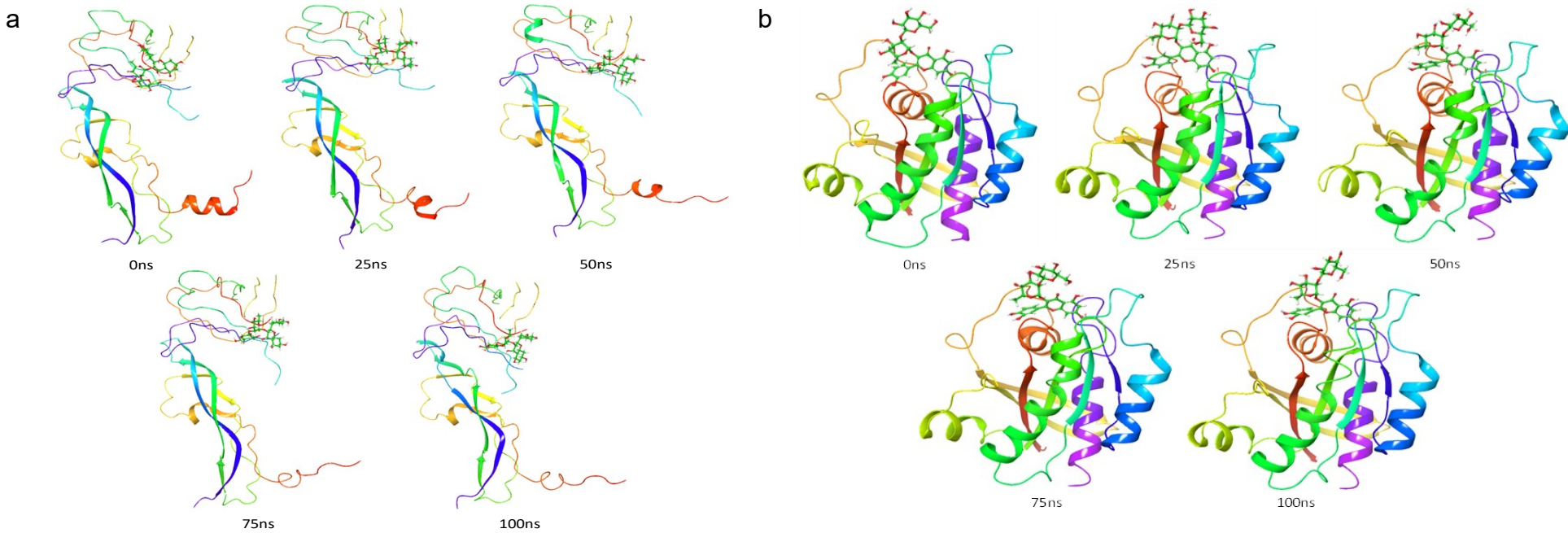

Figure S11. Time series snapshots of MD trajectories to analyze the pose of (C) 4QAF+quercetin 3-O-β-D-glucopyranosyl-(1->2)-rhamnopyranoside and (D) 7JII+quercetin 3-O-β-D-glucopyranosyl-(1->2)-rhamnopyranoside conformational deviation throughout 100 ns time.